

High Resolution X-Ray Diffraction to Characterize Semiconductor Materials

Marcelo Assaoka Hayashi*, Rogério Marcon

Instituto de Física Gleb Wataghin, Unicamp, CP6165, 13083-970, Campinas, SP, Brazil

Danilo Rocha Nunes

FEEC, Unicamp, 13083-970, Campinas, SP, Brazil

marcelo@led.unicamp.br

Abstract

X-ray diffraction gives information on the composition and lattice strain of III-V and II-VI ternary and quaternary heteroepitaxial semiconductor layers used in the fabrication of optoelectronic devices. In this article we give a brief introduction to the materials used in technology of III-V optoelectronics, and how X-ray diffraction can provide vital information to researchers involved in the growth and development of these semiconductor materials.

1 Introduction

Electronics became the basis of the largest industry in the world, being the core for main domains of modern technology, such as computers, telecommunications, control of industrial processes and consumer products. In the heart of an electronic system, the processing unit is the main element, comprising semiconductor devices belonging to one or several integrated circuits (IC's). Research work in physics[1] is needed for technological advance towards IC's with increased speed, complexity and density of integration (ultra large scale integration, ULSI).

Particularly, materials and devices characterization is a key enabler in the development of semiconductor technology and to improve semiconductor manufacturing, especially in the field of compound semiconductors, where inherently complicated materials are being used in increasingly complex structures. On the other side, commercial pressures force prices downward through increased yields and waste elimination. The first solid state transistors were made of Germanium, and nowadays Silicon technology dominates the semiconductor industry. However compound semiconductors from groups III and V of the periodic table, Gallium Arsenide and Indium Phosphide, for example, also have great technological interest. These materials have some unique properties which make them suitable for a number of applications. The III-V's have some advantages over Silicon. Transistors made of GaAs or InP are intrinsically up to ten times faster than those made of Si. Many of the III-V's are direct-gap semiconductors, which means that electrons travel directly between the valence band and the conduction band, and, as they do so, they emit or absorb a

photon of light. Diode lasers can be made from these materials, and the wavelength of the emitted light depends upon the band gap of the material. Most importantly, using very sophisticated growth techniques, highly perfect crystals can be grown with a mixture of elements from groups III and V. A crystal can be grown, for instance, by a mixture of GaAs and AlAs giving AlGaAs. This ternary compound has some extremely useful properties. The pure compounds GaAs and AlAs have different band gaps, and by adjusting the proportions of Ga and Al in the ternary compound, any band gap in the intermediate range can be chosen. In other words, the wavelength of the light emitted by the laser can be tuned, and this fact has important implications on modern optical communication systems.

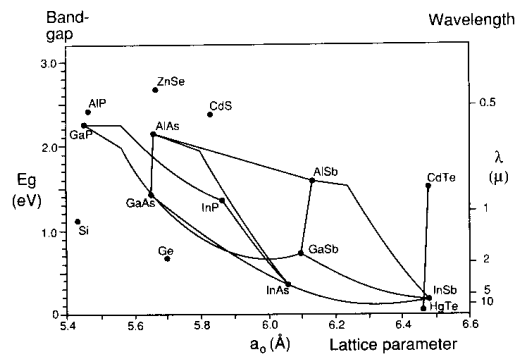


Figure 1: band gap vs. lattice parameter of elemental group IV semiconductors and of III-V and II-VI compound semiconductors.

Figure 1 shows how the band gap (and so the wavelength of emitted or detected light) of the III-V compound semiconductors varies with composition[2]. The

*Present address: Centro de Componentes Semicondutores/UNICAMP

dots on the figure represent the binary compound, such as GaAs, InP, etc. The lines represent the ternary compounds such as GaInP, formed by careful control of the constituent materials during crystal growth. The figure also shows how the lattice parameter of the compound crystals is related to their composition, and this is the link to X-ray diffraction. X-ray diffraction can measure lattice parameters and these can be related to the composition of the material and so to the band-gap.

Careful control of the composition is important. For example, optoelectronic devices are widely used as transmitters or receivers in fiber optic communication systems. Fiber optics have several windows in their transmission spectra at well defined wavelengths, and it is better to tune the characteristics of the emitter and receiver in order to operate at these wavelengths. The technique used to alter the electronic or optical properties of a material, by control of its composition, is known as band-gap engineering.

2 Epitaxial Growth

Figure 2 shows a simplified scheme of a GaAs laser diode structure. It is made up of a number of very thin semiconductor layers of various compositions. The layers are about a micron, or so in thickness and are almost perfectly crystalline.

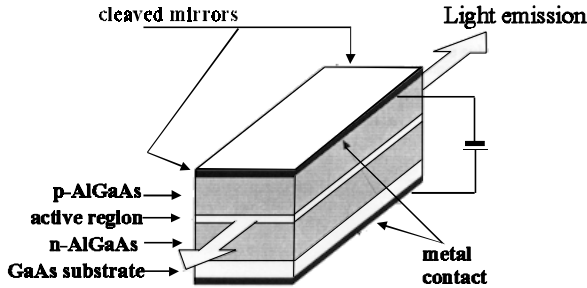


Figure 2: Scheme of laser diode structure[3].

The band-gaps of the various layers are engineered in such a way that, when a voltage is applied to the laser, light is emitted in the active layer, and trapped within it by the change in the refractive index at the interface between the active layer and its surrounding layers. For the laser to work correctly, the composition of the layer must be adjusted to give the right wavelength, and also there must be few defects in the crystal structure, as these trap the photons and reduce the device efficiency. Therefore the crystal layers must be grown under extreme careful control of thickness and composition, starting over a crystalline base or substrate. This process is known as epitaxy.

Epitaxial growth means to start with a substrate, and adding atoms to the crystal one by one so that a crystalline layer grows onto the substrate. The arrangement of the atoms is continuous across the interface between the substrate and the layer.

The last decade has witnessed an enormous progress in epitaxial growth technologies. Growth methods like Molecular Beam Epitaxy (MBE), Metal-Organic Vapour Phase Epitaxy (MOVPE), Hot Wall Epitaxy (HWE), Liquid Phase Epitaxy (LPE) and their variants are nowadays mature and applicable for device fabrication. Using these techniques a large number of different combinations of semiconductors have been successfully deposited onto various substrate materials.

All these techniques have one common objective: to produce perfect controlled composition and thickness.

3 X-Ray Diffraction

In figure 1 we saw that there was a simple relationship between the lattice parameter of a ternary compound semiconductor and its band-gap and composition. X-ray Diffraction is good for measuring lattice parameters, and this forms the basis of the High Resolution X-ray Diffraction analysis.

The foundation of all X-ray diffraction analysis is the Bragg law[4]:

$$n \cdot \lambda = 2 \cdot d \cdot \sin \theta \quad (1)$$

Where the integer n is the order of the corresponding reflection, λ is the X-ray wavelength, d is the lattice interplanar spacing and θ the angle of incidence. Deriving this expression, taking $\Delta\lambda = 0$ (monochromatic radiation), leads to:

$$\frac{\Delta d}{d} = -\cot \theta \cdot \Delta \theta \quad (2)$$

hence, the difference of layer/substrate lattice parameters can be measured.

For example, taking a simple single-layer epitaxial structure, we can see that if layer and substrate compositions differ, also do their lattice parameter. If we illuminate the sample with a parallel, monochromatic X-ray beam, and then slowly rotate the sample through the Bragg angle θ , the substrate will diffract at one angle and the layer at another, as in figure 3.

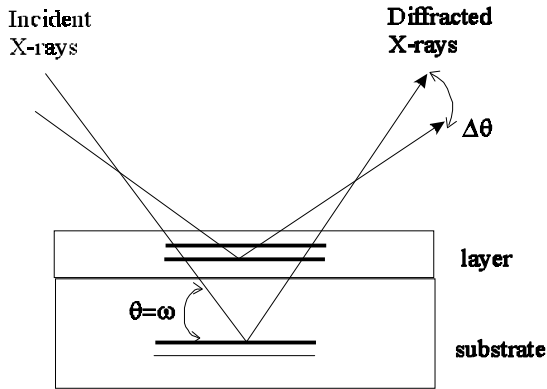


Figure 3: Diffraction from epitaxial layer and substrate.

Recording the diffracted intensity as a function of the angle, we obtain the diffraction pattern depicted in figure 4. For historical reasons, this is commonly called a “rocking-curve” or ω scan.

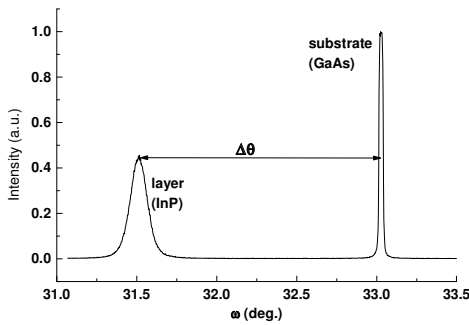


Figure 4: Rocking-curve of an InP layer over GaAs substrate.

We extract information from the rocking-curve following some steps:

We KNOW the lattice parameter of the substrate;

We MEASURE the angular separation of substrate and layer peaks, $\Delta\theta$;

We CALCULATE the difference between substrate and layer lattice parameters, with equation (2);

We CALCULATE the layer lattice parameter.

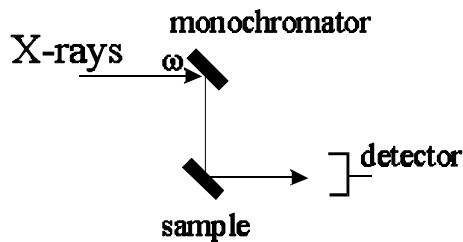
From the relationships between lattice parameter and composition illustrated in figure 1 we can now calculate the composition of the layer.

This outlines the basic principles lying behind “rocking-curve” analysis. But, in reality, things are more complicated than this and high resolution X-ray diffraction contains much more useful data.

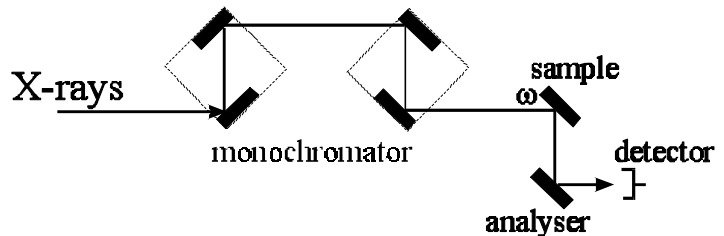
4 Rocking-curves in a double crystal system

The most familiar form of high resolution X-ray technique for semiconductors is the rocking-curve technique[5, 6]. It is normally undertaken on a double crystal diffractometer (fig. 5a). The purpose of the first crystal is to remove wavelength dispersion, acting as a monochromator/collimator, before the sample or the second crystal. In order to achieve the highest resolution, we have to work with the non-dispersive arrangement, when both the first crystal and the sample are of the same kind, and aligned in the same reflection geometry. This is a significant disadvantage, because it will require complete realignment if we want to study more than one reflection or material. To overcome this problem, a more sophisticated setup is now commercially available, with a two-crystal and four reflections monochromator and a analyzer crystal, the so called four-crystal six-reflection diffractometer [7] (fig. 5b).

The results shown in this work were performed in the double-crystal system of Laboratório de Difração de Raios-X/IFGW/Unicamp [8].



(a)



(b)

Figure 5: Schematic of (a) double and (b) four crystal diffractometers. Monochromator crystals in (b) have a “U” shape cut (for two reflections in the same crystal), called channel-cut.

5 Dynamical Theory Of X-Ray Diffraction

Besides the characterization of layer parameters including layer composition, mismatch and thickness, more sophisticated characterization of interfaces, quantum-well and superlattice structures (multilayer structures) is only possible with the diffraction simulation using the dynamical diffraction theory.

The X-ray diffraction theory for distorted crystals was developed in the 1960s by Takagi [9] and Taupin [10]. This theory is a first-order approximation to the Maxwell (or Schroedinger) wave equation for an X-ray (or electron) wave propagating in a distorted crystal medium. The so called Takagi-Taupin equation is a system of coupled linear partial differential equations for the incident and diffracted amplitudes, and describes the interchange of energy between the two amplitudes as they propagate in the crystal medium, and therefore it is a dynamical theory. Rocking-curves are calculated by solving the Takagi-Taupin equations [11, 12], which give the rate of change of the ratio of diffracted to incident beam amplitudes, as a function of depth below the surface. For a single homogeneous layer the equation can be solved analytically, giving the amplitude ratio at one surface relative to that at another. In order to apply this to heteroepitaxial structures we must consider each sample as subdivided into layers of constant lattice parameter and structure factor. By matching the amplitude at the substrate surface to that at bottom of the epitaxial layers, the amplitude of the beam at the surface can be numerically evaluated. The reflectivity of the sample is given by the square of the modulus of the amplitude. The reflectivity curve of the sample is convoluted with the reflectivity curve of the first crystal (monochromator) used in the double crystal diffractometer to give the rocking-curve. The structure factors for ternary layers are calculated assuming a linear relationship between lattice parameter and composition. Structure factors for quaternary layers have been calculated from the energy gap variation alone, but it is beyond the scope of this work.

When a mismatched epitaxial layer is grown onto a substrate, the substrate will assume an overall curvature which increases with increasing layer thickness and layer mismatch. This curvature leads to a peak broadening, that can be simulated, enabling determination of sample curvature from experimental rocking-curves. The calculations assume that all samples are defect free, but in practice we are dealing with nearly perfect crystals, which usually contain some linear defects called dislocations. Dislocations are essential in explaining the observed strength (or rather, the lack of shear strength) of real crystals, and the observed rates of crystal growth.

We never expect epitaxial layers to be more perfect than the substrate material on which they are grown. This is

because the layer nucleates in an orderly manner, then the interface will be coherent and dislocations in the substrate will be replicated in the layer. Commercially available substrates have dislocation densities up to $10^4/\text{cm}^2$. The dislocations will cause the lattice planes to be tilted, which potentially cause rocking-curve broadening, situation that can be treated in the same way as an overall curvature for simulation purposes.

If growth didn't nucleate so well, there can be large densities of extra dislocations and planar defects in the layer that also can lead to appreciable peak broadening. This broadening would be expected to be symmetrical, unlike the asymmetrical broadening observed when a compositional gradient within is present.

Simulated rocking-curves of a single perfectly flat $\text{Al}_{0.5}\text{Ga}_{0.5}\text{As}$ epitaxial layer on a GaAs substrate with different thickness appear in figure 6 ($t = 2000\text{\AA}$, 5000\AA and 10000\AA), where we can distinguish two large peaks due to the layer and the substrate. We can also observe oscillations (finite thickness fringes, similar to optical Fraunhofer diffraction by a slit). These fringes are typical of samples with good layer/substrate interface, and missing of this fringe pattern is the main evidence of defects in the interface. The intensity of the peaks relates to the scattering matter and the volume sampled, whilst the oscillation period relates to the thickness of the layer. We can clearly see the difference in the profiles due to the layer thickness.

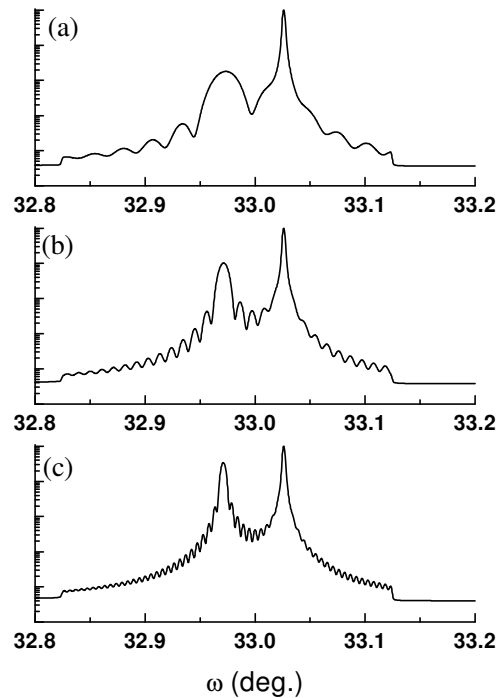


Figure 6: Simulated rocking-curves of a single perfect flat $\text{Al}_{0.5}\text{Ga}_{0.5}\text{As}$ epitaxial layer on a GaAs substrate, with different thickness, (a) 2000\AA , (b) 5000\AA and (c) 10000\AA .

The separation of the two large peaks is related to the difference (mismatch) in the lattice parameters of the layer and substrate. Figure 7 shows the effect of composition ($x = 0.4, 0.5, 0.6$) on the layer peak position, for single perfectly flat $\text{Al}_x\text{Ga}_{1-x}\text{As}$ layers with 5000\AA .

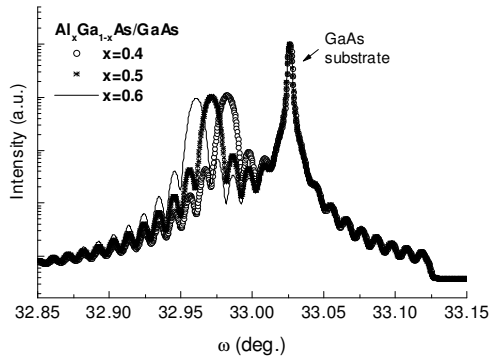


Figure 7: Effect of composition ($x = 0.4, 0.5, 0.6$) on the layer peak position, for single perfect flat $\text{Al}_x\text{Ga}_{1-x}\text{As}$ layers with 5000\AA .

These profiles, figures 6 and 7, contain a considerable amount of information, and simply using the Bragg's law will only give periodicities (lattice parameters and other lengthscales), and unfortunately, considerable errors. Ideally, the profiles should be simulated not only to aid interpretation, but to extract more information.

6 Experimental

Here we show some examples of rocking-curves measured in the double crystal system implemented at Laboratório de Difração de Raios-X/IFGW/Unicamp. Since all the samples have GaAs substrate, for higher resolution non-dispersive setup the first crystal also is a GaAs crystal. X-rays are provided by a microfocus generator with Cu anode ($\lambda = 1.54056 \text{\AA}$). Both crystals are aligned at 004 reflection.

We studied samples of $\text{Al}_x\text{Ga}_{1-x}\text{As}$ grown by Molecular Beam Epitaxy on GaAs substrates [13]. Actually, the samples have a thin (500\AA) AlAs layer between GaAs and AlGaAs and a GaAs (50\AA) layer over the AlGaAs layer. The samples were grown with nominal Al compositions $x = 0.41$ (sample #1) and $x = 0.44$ (sample #2). Nominal thicknesses were 1800\AA and 3700\AA , respectively.

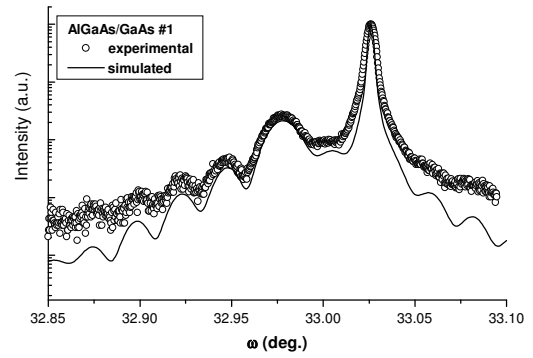


Figure 8: Measured and calculated rocking-curve of $\text{Al}_{0.43}\text{Ga}_{0.57}\text{As}(1750\text{\AA})/\text{GaAs}$.

Figures 8 and 9 show measured and simulated rocking-curves for these samples.

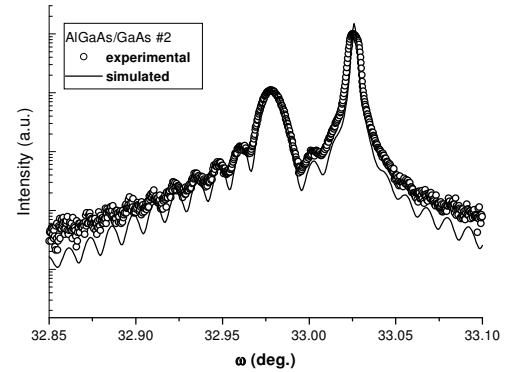


Figure 9: Measured and calculated rocking-curve of $\text{Al}_{0.45}\text{Ga}_{0.55}\text{As}(3800\text{\AA})/\text{GaAs}$.

From the fitting between measured and calculated curves, we got slightly different values from the expected ones. Sample #1 has 43% ($x = 0.43$) of Al, and the layer is 1750\AA . Sample #2 has a 3800\AA layer with 45% Al.

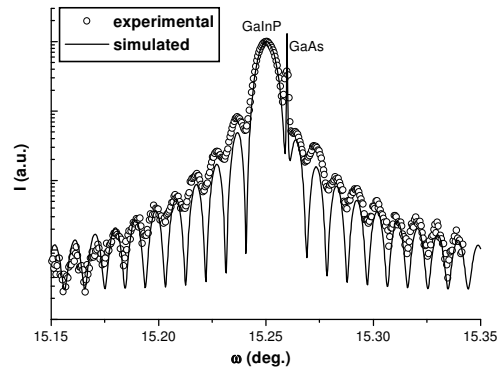


Figure 10: Measured and calculated rocking-curve of $\text{Ga}_{0.51}\text{In}_{0.49}\text{P}(4700\text{\AA})/\text{GaAs}$.

Figure 10 shows the rocking-curve of a $\text{Ga}_x\text{In}_{1-x}\text{P}$ layer over a GaAs substrate [14], aligned at 002 reflection. This sample was grown by Chemical Beam Epitaxy at LPD/IFGW/Unicamp. The measurements were carried out during the commissioning of the new station 16.3 (High Resolution Single Crystal Diffraction) of Synchrotron Radiation Source, Daresbury Laboratory, Warrington, UK. This station is sited 32 m from a 6 tesla superconducting wavelength-shifter. Highly collimated, un-focused X-rays are monochromatized by a Si 111 water-cooled channel-cut crystal to provide a tunable ($\lambda \approx 1.4704 \text{ \AA}$ in this case) beam at the sample position. After the fitting between measured and calculated data, we got layer composition of 51% of Gallium and 4700 \AA for thickness.

Another example is the study of damage caused by ion implantation in semiconductor crystals. Ion implantation is the main technique to achieve controlled doping of semiconductors. In very simplistic terms, the species to be implanted are ionized and undergo an acceleration, up to 200 keV in a conventional implanter, to achieve the desired penetration depth in the semiconductor. We studied GaAs wafers [15] submitted to Si^+ implantation at various energies and doses at Centro de Componentes Semicondutores-CCS/Unicamp. Figure 11 shows the rocking-curve of a GaAs substrate implanted with Si^+ at 80 keV and $2 \times 10^{13} \text{ ions/cm}^2$. With the simulation, we can get the strain profile (inset figure 11) in the sample, showing the damage due to the displacement of lattice atoms caused by the ions collision. This strain profile is related to the ion concentration with depth.

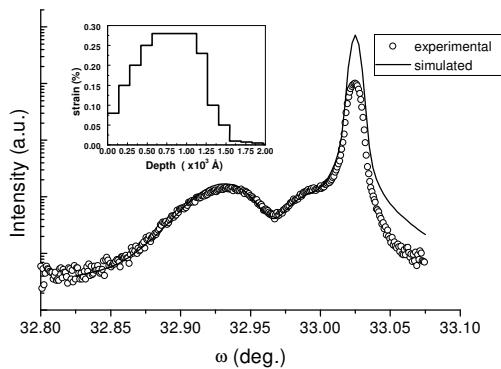


Figure 11: Measured and calculated rocking-curve of a GaAs wafer submitted to Si^+ implantation (80 keV , $2 \times 10^{13} \text{ ions/cm}^2$). The inset shows the strain profile obtained from the simulation.

7 Conclusion

With the advances in the epitaxial growth techniques and due to the importance of knowing the structural characteristics of epitaxial layers for application in high performance electronic and optoelectronic integrated-circuit technology, the X-ray rocking-curve technique has

become an essential and versatile tool for characterizing heteroepitaxial structures. It offers a powerful, relatively quick, non-destructive means of assessing epitaxial layers characteristics. The method is well established for routinely measuring the lattice parameter difference between epitaxial layers and their substrates. By comparing experimental and theoretical curves it is possible to deduce several more layer parameters. For layers with good crystalline quality it is possible to get the layer thickness and to detect variations in the composition of the layers with depth. For less perfect layers an estimate of layer quality can be made from the peak width. For ion implanted semiconductors, the strain profile with depth can be estimated from the simulation.

The structural information from the rocking-curve data is often complementary to the information obtained from transmission electron microscopy (TEM) data, or from photoluminescence (PL) spectroscopy data. By combining the X-ray rocking-curve and PL characterizations (both non-destructive) with the electrical and device studies, or in other words, by correlating the growth, structural, electro/optical and device properties, one can try to optimize the growth process for the device structure of interest.

Here we presented a brief description of some aspects of X-ray rocking-curve characterization, and discussed a few examples of measurements performed in the double-crystal system implemented for routine analysis, together with other more sophisticated techniques, available at Laboratório de Difração de Raios-X/IFGW/Unicamp.

The authors wish to acknowledge J. Bettini, M. M. G. de Carvalho, L. H. F. de Andrade, J. M. Sasaki and L. C. Kretly for the samples used in this work. The authors also thank CNPq and FAPESP for financial support.

8 References

- [1]G. Kamarinos & P. Felix, J. Phys. D: Appl. Phys. **29**, 487 (1996).
- [2]G. Bauer & W. Richter in: Optical Characterization of Epitaxial Semiconductor Layers, G. Bauer & W. Richter, eds. Springer, Berlin 1996.
- [3]T. W. Ryan, Materials Research Society short course C.23, 1990.
- [4]N. W. Ashcroft & N. D. Mermin in: Solid State Physics, Holt, Hinehart and Winston, Orlando 1976.
- [5]P. F. Fewster, Semicond. Sci. Technol. **8**, 1915 (1993).
- [6]C. R. Wie, Mater. Sci. Eng. R **13**, 1 (1994).
- [7]P. F. Fewster, J. Appl. Cryst. **22**, 64 (1989).
- [8]J. M. Sasaki, M. A. Hayashi, A. P. Pereira, S. L. Morelhão & L. P. Cardoso, Engenharia e Ciência dos Materiais (Anais do X Congresso Brasileiro, vol I.), Campinas-SP, Universidade de Campinas, 1992.
- [9]S. Takagi, Acta Cryst. **15**, 1311 (1962).

- [10]D. Taupin, Bull. Soc. Fr. Minéral Cryst. **87**, 469 (1964).
- [11]W. J. Bartels, J. Hornstra & D. J. W. Lobeek, Acta Cryst. A **42**, 539 (1986).
- [12]A. Pesek, P. Kastler, L. Palmetshofer, F. Hauzenberger, P. Zuza, W. Faschinger & K. Lishcka, J. Phys. D: Appl. Phys. **26**, A177 (1993).
- [13]Leandro H. F. de Andrade, Tese de Doutorado, IFGW/Unicamp, 1998.
- [14]M. A. Hayashi, L. H. Avanci, L. P. Cardoso, J. Bettini, M. M. G. de Carvalho, S. L. Morelhão & S. P. Collins, J. Synchrotron Rad. **6**, 29 (1999).
- [15]M. A. Hayashi, C. Campos, L. P. Cardoso, J. M. Sasaki & L. C. Kretly, Pesq. Desenv. Tecnol. **19**, 49 (1995).